Ecological Indicators 60 (2016) 125–136

Contents lists available at ScienceDirect

Ecological Indicators

journal homepage: www.elsevier.com/locate/ecolind

Magnetic properties of *Tillandsia recurvata* L. and its use for biomonitoring a Mexican metropolitan area

Ana G. Castañeda Miranda[a], Marcos A.E. Chaparro[b,*], Mauro A.E. Chaparro[b,c], Harald N. Böhnel[a]

[a] Centro de Geociencias, UNAM, Blvd. Juriquilla 3001, 76230 Juriquilla, Querétaro, Mexico
[b] Centro de Investigaciones en Física e Ingeniería del Centro de la Provincia de Buenos Aires (CIFICEN, CONICET-UNCPBA), Pinto 399, 7000 Tandil, Argentina
[c] Departamento de Matemáticas, Facultad de Ciencias Exactas y Naturales UNMDP, Mar del Plata, Argentina

ARTICLE INFO

Article history:
Received 31 July 2014
Received in revised form 15 June 2015
Accepted 18 June 2015

Keywords:
Atmospheric pollution
Bioindicator
Magnetic properties
Monitoring
Magnetite

ABSTRACT

Some epiphytic species accumulate airborne particles and are suitable biological indicators for monitoring urban and industrial pollution. The species *Tillandsia recurvata* L. was studied as a monitor of air pollution in an urban area from Mexico. Individuals were collected in 25 sites which are exposed to different pollution degree and sources.

The magnetic particle concentration, particle size, and mineralogy were determined and compared with chemical contents for all samples. The highest values of magnetic concentration dependent parameters were observed in industrial and heavy traffic sites (e.g., mass specific magnetic susceptibility of up to $171.5 \times 10^{-8}\ m^3\ kg^{-1}$). In contrast, sites with low or without vehicular traffic reached low values (e.g., mass specific magnetic susceptibility of down to $1.8 \times 10^{-8}\ m^3\ kg^{-1}$). The integrated magnetic analysis (King's and Day's plots, remanent magnetization parameters and thermomagnetic measurements) revealed the presence of ferromagnetic minerals, mostly magnetite-like with fine grain sizes (0.1–1 μm) and subordinate presence of high-coercivity minerals. Selected samples were observed by SEM and EDS analysis and revealed the presence of Fe-rich particles, as well as trace elements, among others, As, Sb, S, Cr, Mo, V, Zn, Ba, Hg, Pt and Cu. Most of the elements detected by EDS were also quantified by ICP-MS measurements.

Multivariate statistical analyses prove a high correlation between magnetic parameters and elements, as well as allow us classifying sites in clusters (fuzzy c-means clustering) with different pollution degree. These results demonstrate the usefulness of the species *T. recurvata* L. as a passive pollution monitor, with an affordable and immediate application. This species is abundant not only in Mexico, but also in other cities from America.

1. Introduction

Magnetic monitoring is an appropriate technique to assess, as first approach, the influence of anthropogenic pollution in areas of interest (Petrovský and Elwood, 1999). In general, the atmospheric dusts in urban/industrial areas are collected using filters. This technique requires a strategic distribution of several devices in the area, which need to be maintained resulting in high cost and time investment. Environmental magnetism studies of dust collected by filters have been reported in European (Muxworthy et al., 2001; Sagnotti et al., 2006), Asian (Xie et al., 2001; Shu et al., 2001), and American (Castañeda-Miranda et al., 2014) cities.

In contrast, biological monitors are an advantageous alternative to monitor the air quality in urban areas. In particular, they do not need any special care and their collection time may vary between days to years according to the species used. Recently, several authors have demonstrated the capacity of some biomonitors (needles, tree leaves, tree ring cores, mosses and lichens) to suit as dust collectors, and they were used for magnetic monitoring of air quality (Lehndorff et al., 2006; Maher et al., 2008; Zhang et al., 2008; Jordanova et al., 2010; Fabian et al., 2011; Salo et al., 2012; Chaparro et al., 2013).

Tillandsia recurvata L. is an epiphytic plant of about 8 cm radius in average, which has a basic root system and usually has a spheroid shape (Madison, 1977). These plants have foliar trichomes that allow absorbing water, nutrients and dusts from the air (Rzedowski, 1981); they can colonize trees and cables and are available and well distributed in America, from the southern United States to the

* Corresponding author. Tel.: +54 249 4385661; fax: +54 249 4385669.
E-mail address: chapator@exa.unicen.edu.ar (M.A.E. Chaparro).

http://dx.doi.org/10.1016/j.ecolind.2015.06.025
1470-160X/

south Argentina and Chile (Correll and Johnston, 1970). The northernmost limit of its natural occurrence is coastal Georgia (where it is listed as a State "Special Concern" species), although it has been introduced into coastal South Carolina on landscaping trees. It has been reported in nature from Georgia, Florida, Louisiana, Texas, Arizona, Mexico, most of Central and South America, and many of the islands in the West Indies (Weakley, 2010). These characteristics and the distribution of the species allow studying its ability as collector of different pollutants, such as toxic elements, particulate matter (e.g., Shacklette and Connor, 1973; Schrimpff, 1984; Brighigna et al., 1997; Graciano et al., 2003; Fonseca et al., 2007; Goix et al., 2013) and magnetic oxides. Monitoring studies using transplanted individuals of *Tillandsia* spp. reported by different authors trace element accumulation for minimum time periods of 4 weeks (Pellegrini et al., 2014), as well as for 3–9 months (Bermudez et al., 2009; Abril et al., 2014).

In this study, the *T. recurvata* was investigated as collector of atmospheric dusts (magnetic particles and toxic elements) and its suitability for monitoring an urban area by measuring their magnetic properties. Among other available collectors in cities (e.g., urban soils, filters, river sediments, etc.), this biological species has diamagnetic properties at difference to industrial/urban pollutants (para, antiferro and ferrimagnetic properties). This fact makes it as an interesting recorder of magnetic pollutants. In addition, it is well-known that magnetic particles produced by pollution (industrial/urban) sources can act as host of heavy metals and other non-magnetic pollutants including them onto its crystalline structure or on its surface (e.g., Kukier et al., 2003; Chaparro et al., 2010). Therefore, magnetic measurements may be able to assess the adverse effects of anthropogenic activities over time. Our work is focused on the use of *T. recurvata* as an alternative bioindicator in cities, and to determine relevant parameters for magnetic monitoring. It is worth mentioning that the magnetic monitoring is a fast and low cost methodology applicable wherever the species can be recollected, and this way allows identifying contamination hotspots and critic areas for further complementary studies (e.g., Böhm et al., 1998; Moreno et al., 2003; Chaparro et al., 2013).

In particular, this work aims to investigate: (1) the potential use of *T. recurvata* as suitable dust collector, including magnetic particles; (2) the relationship between magnetic particles and chemical elements accumulated in this species; (3) the use of magnetic parameters measured in *Tillandsias* for spatial and temporal biomonitoring in urban areas.

2. Sampling and laboratory methods

2.1. Study area

Santiago de Querétaro (or Querétaro for short) city is the capital of Querétaro de Arteaga state from Mexico. It is located in the central Mexico volcanic highlands (20° 36′ N; 100° 24′ W) at about 1820 m a.s.l. (INEGI, 2006). The urban area covers about 741 km^2 and has ~800,000 inhabitants but neighboring municipalities raise the population of the urban area to approximately one million (SEDESU, 2011).

The main sources of air pollution comprise vehicular traffic (automobiles and trucks), contributing about 75% of pollutants. For the city, registered vehicles reached 195,000 in 2010, with an annual growth rate of about 8% (INEGI, 2010). The higher abundance of Fe particles in the city center and the higher magnetic susceptibility values observed there suggest that vehicle emissions are an important source of pollution (Castañeda-Miranda et al., 2014). In addition, the industrial activities also contribute to air pollution according to Gasca (2007). Additional information is available in Supplementary data.

2.2. Sampling

About three individuals of *T. recurvata* were collected from 25 sites (a total of 70 samples) from the urban area and the outskirts, some of them with higher pollutant loadings, as well as influenced by different pollution sources (Fig. 1). For the sampling design, the city was subdivided into 25 squares of 4 km^2, including industrial, urban and outskirt areas. Within each square, a sampling point was chosen according to the availability of *Tillandsias*. Most of the sites are located along main streets and avenues where *T. recurvata* were often found on the *Prosopis laevigata* and *Acacia farnesiana* trees planted on the sidewalks (less common on *Shinus molle* and *Bursera fagaroides* trees). Both are endemic species and have a high relative abundance (25%) in Querétaro city (Castañeda-Miranda, 2015).

Samples were collected at a height of >1.5 m to avoid the influence of urban soil particles; moreover plastic scrapers and disposable gloves were used to avoid possible contamination with tools and between collection sites. As this plant is a composite of leaves of different ages, specimens of similar age were collected in order to avoid important differences in exposure periods, by choosing about 10–12 cm diameter size. All material was collected in March 2012, packed in paper bags and stored at room temperature in the laboratory before magnetic and other studies.

2.3. Magnetic measurements

Biological material was packed into nonmagnetic plastic containers (8 cm^3) and weighed (up to 3.2 g) for magnetic measurements. All rock-magnetic measurements were carried out in the Laboratory of Paleomagnetism and Rock-magnetism at Centro de Geociencias (UNAM).

A small amount of plant material (<50 mg) was used to measure magnetic hysteresis loops and remanent magnetizations in fields between −2 and 2 T at room temperature using a Princeton Measurement Corporation Micromag 2900 AGM system. Before the experiments, the material was dried and weighed to allow for calculation of mass-corrected hysteresis parameters. Among hysteresis parameters and ratios of interest, the saturation magnetization (M_s), saturation remanence (M_{rs}) and coercive force (H_c) were calculated. In addition, the high-field magnetic susceptibility (χ_{hf}) and the relative contribution of paramagnetic and diamagnetic minerals to the M_s (para/diamag. cont.) were calculated. From remanent measurements, IRM acquisition curves and the saturation of IRM (SIRM = IRM_{2T}) were determined using forward DC fields equally spaced on a logarithm scale. Remanent coercivity (H_{cr}), *S*-ratio (=$-IRM_{-300mT}$/SIRM), ARM/SIRM and SIRM/κ ratio were also calculated.

Selected samples (of about 100–220 mg) were studied in a laboratory built horizontal magnetic balance to produce thermomagnetic curves. The induced field was chosen at 0.5 T, and ramp-rates during heating and cooling were 30 °C min^{-1}. Samples were heated in air to a temperature of about 700 °C and subsequently cooled to room temperature (RT). The relative values of induced magnetization (M/M_{RT}) are of interest in this study; hence the $M/M_{RT} - T$ curves are presented.

Measurements of low-field magnetic susceptibility, volumetric (κ) and mass-specific (χ), were carried out using a KLY-3 meter (AGICO). Also, the frequency-dependence of magnetic susceptibility κ_{FD}% ($\kappa_{FD}\% = 100 \times [\kappa_{0.47} - \kappa_{4.7}]/\kappa_{0.47}$) was computed from measurements with a MS2 (Bartington Instruments Ltd.) instrument linked to the MS2B dual frequency sensor (0.47 and 4.7 kHz).

Anhysteretic remanent magnetization (ARM) was imparted using a laboratory built alternating field (AF) demagnetizer by superimposing a DC bias field of 90 μT to an alternating magnetic field of 100 mT amplitude, and the ARM was measured with an induction magnetometer (JR-5, AGICO). Anhysteretic susceptibility

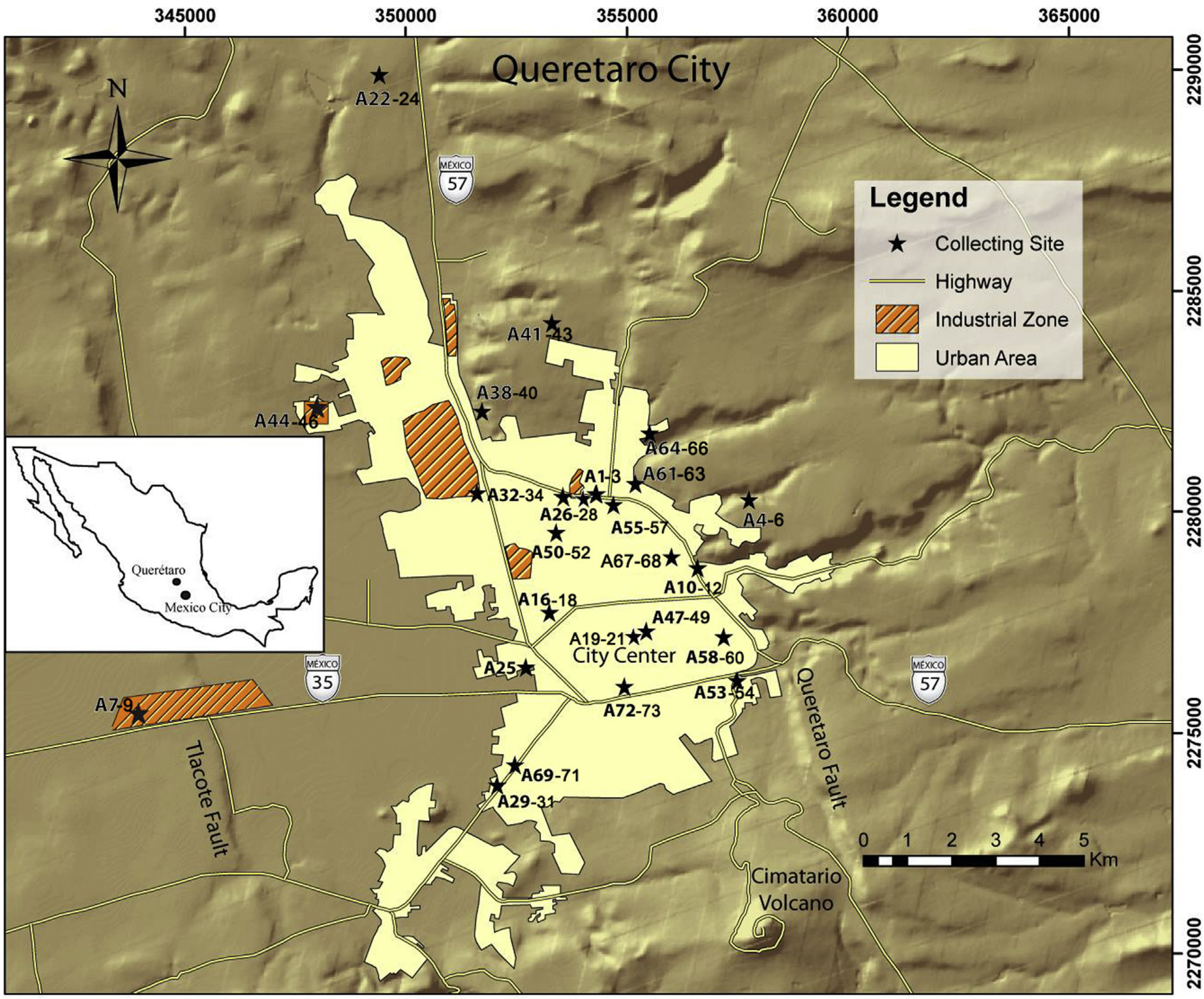

Fig. 1. Map of Querétaro area (México). The main traffic street ways (highways and streets), industrial zones, urban areas and 25 sampling sites area are shown.

(κ_{ARM}) was estimated from the ARM acquired in this DC bias field. The κ_{ARM}/κ-ratio and the King's plot (χ_{ARM} versus χ, King et al., 1982) were also studied.

Saturation of isothermal remanent magnetization (SIRM) was also produced using a pulse magnetizer by applying a field of 2 T, and measured using the JR-5 magnetometer.

2.4. Microscopy and elemental studies

Several samples of unmodified *Tillandsias* were examined by scanning electron microscopy (SEM) using a Phillips microscope, model XL30. This microscope also allowed to analyze the elemental composition of each specimen by X-ray energy dispersive spectroscopy (EDS) with an EDAX model DX4 (detection limit 0.5%). Trace element data were obtained by inductively coupled plasma mass spectrometry (ICP-MS) using the Thermo Scientific™ iCAP™ Qc ICP-MS at the Centro de Geociencias at the UNAM, following the sample preparation and measurement procedures described by Mori et al. (2009) (detailed information in Supplementary data).

2.5. Multivariate analysis

Multivariate statistical analyses were performed using the free software: R version 2.15.0 (2012). Twenty-five samples were used for this investigation and the data set included 13 magnetic variables (χ, ARM, SIRM, Ms, κ_{ARM}/κ, ARM/SIRM, SIRM/χ, H_c, H_{cr}, H_{cr}/H_c, M_r/M_s, para/diamag cont. and χ_{hf}) and 11 chemical variables (V, Cr, Co, Ni, Cu, Zn, Mo, Sn, Sb, Ba and Pb). The descriptive statistics and Pearson's correlation coefficients for all variables and data were calculated as a first step. Then, the fuzzy c-means clustering (FCC) method was used to determine clusters (see Chaparro et al., 2012).

3. Results and discussion

3.1. Magnetic properties

Results of magnetic concentration and mineralogy dependent parameters are listed in a Table as Supplementary data. For each site, mean value (s.d.) of χ, ARM, SIRM, χ_{ARM}, κ_{ARM}/κ, ARM/SIRM and SIRM/χ were computed to obtain a representative value.

Mass specific magnetic susceptibility and remanent magnetic parameters are significantly correlated (e.g., $R = 0.976$, $p < 0.01$ for χ-SIRM; $R = 0.949$, $p < 0.01$ for χ-ARM) revealing that the magnetic signal is produced mainly by ferromagnetic materials. The magnetic concentration dependent parameters show wide variations, e.g., χ values varied from 1.8 (0.2) to 171.5 (13.0) $\times 10^{-8}$ m^3 kg^{-1}, for site A41-43 and A1-3, respectively; these sites are characterized by different pollution sources. The influence of different

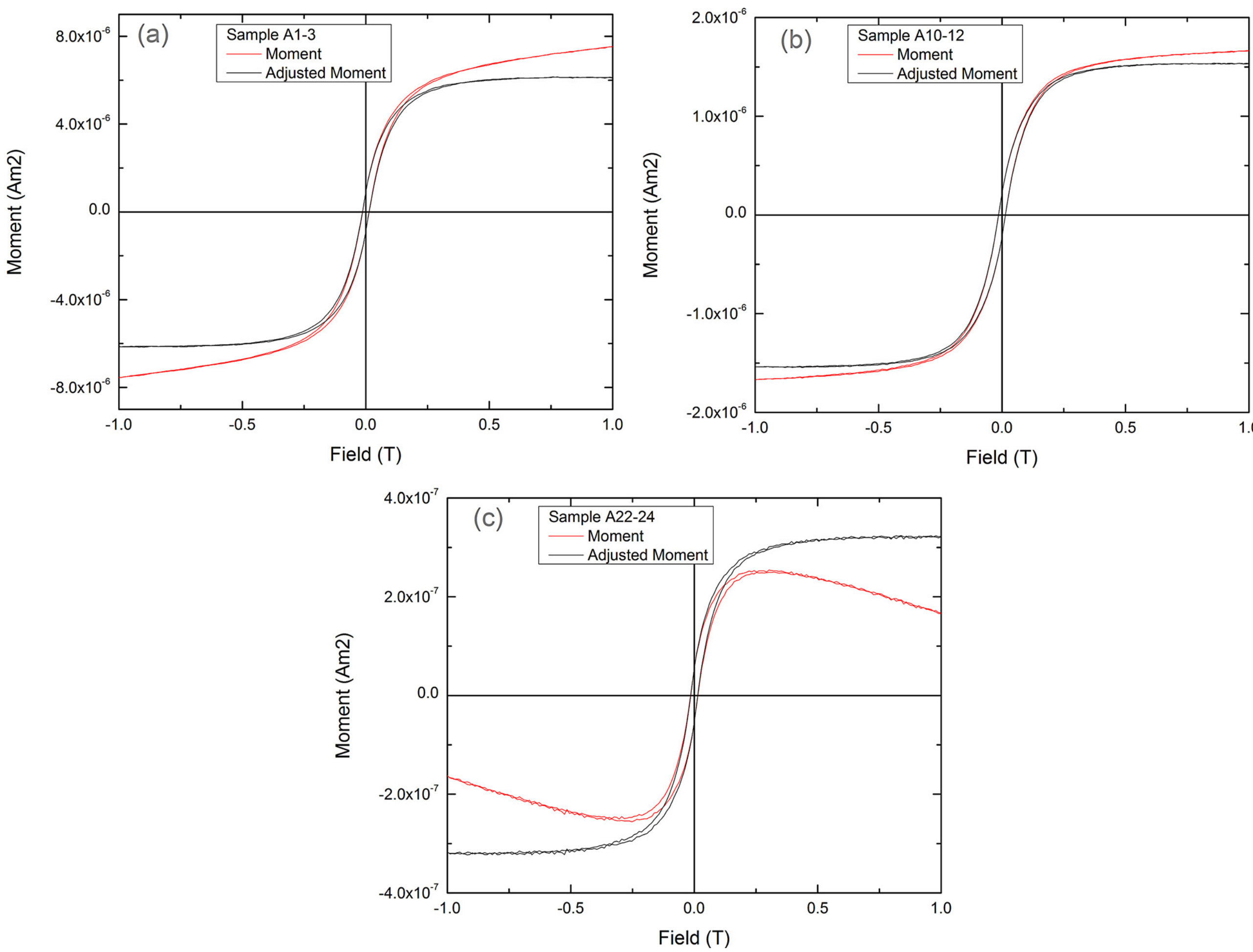

Fig. 2. Characteristic hysteresis curves for selected sites. Corrected (adjusted) curves for the paramagnetic and diamagnetic contributions are in black. Samples correspond to monitoring sites close to the industrial zone: site A1-3 (a), in the city center: site A10-12 (b) and control site: site A22-24 (c). Note the paramagnetic contribution for figures a and b in contrast to the diamagnetic contribution for figure c.

pollution sources is observed in the magnetic hysteresis signal of three selected samples belonging to industrial, urban and control sites. Hysteresis curves from a site close to a factory (Fig. 2a, site A1-3) and another one influenced by high traffic (Fig. 2b, site A-10-12), both show a predominant ferrimagnetic component (H_c = 13.4–13.9 mT) and a paramagnetic contribution of 11.5–4.3% at 1 T. A control site (site A22-24) far away from factories and the urban area shows evidence of a lower magnetic moment (Fig. 2c) than other sites, and is dominated by the natural characteristics of the biological material with an important diamagnetic contribution (−24.2% at 1 T). In this case, the lithogenic contribution is mainly ferrimagnetic (H_c = 14.3 mT) and the diamagnetic matrix (corresponding to the *Tillandsia* spp.) is clearly evident in the uncorrected hysteresis curves.

The high-field susceptibility is a parameter related to the dia- and/or paramagnetic mineral phases, with χ_{hf} values ranging from -2.1 to 9.0×10^{-8} m^3 kg^{-1}. These values correspond to the occurrence of diamagnetic materials (minerals and plant material) from less polluted and paramagnetic (e.g., Fe-rich) materials from polluted sites.

According to the remanent coercivity values (H_{cr} = 35.3–43.9 mT), the ferrimagnetic phase corresponds to magnetite/maghemite minerals. While this parameter varied within a narrow range, there is a notable increase in sites with high magnetic concentration, Possibly the presence of a subordinate magnetic mineral and/or changes in the particle grain size distribution are responsible for this increase.

Both possibilities seem possible according to additional data available. Thermomagnetic curves show the dominance of magnetite-like minerals for all samples (Fig. 3), but samples from sites close to factories also evidenced a phase corresponding to hematite with a high Curie temperature ($T_N \sim 675\,°C$), which also has a high-coercivity H_{cr}. This additional magnetic phase may explain the H_{cr} variation between sites affected to different degree by pollution. Moreover, this phase seems to be a characteristic magnetic phase from industrial sources as it was also reported by Chaparro et al. (2013) in Argentina using lichens as biomonitors.

The magnetic grain size distribution can be appreciated in Fig. 4. In the Day's plot (Fig. 4a) all samples fall into the field of pseudo single domain (PSD) grains, but it is evident that they correspond to different mixture of SD and MD particles, with a MD contribution ranging between 70 and 85% (as based on the SD-MD mixing curves of Dunlop, 2002a,b). Three previously heated samples which were used for thermomagnetic measurements are also shown in Fig. 4a (identified as: ih, iih, iiih), which allows to estimate heating induced changes of the magnetic minerals. All data points move toward the SD part of the mixing curves and thus suggest a reduction of particle grain size.

Analyzing the King's plot (Fig. 4b) we suggest that coarser magnetic grains seem to be associated to higher values of χ. Assuming the dominance of magnetite-like minerals, they would vary between <0.1 and 1 μm and thus comprise a breathable fraction with potentially adverse consequences for human health.

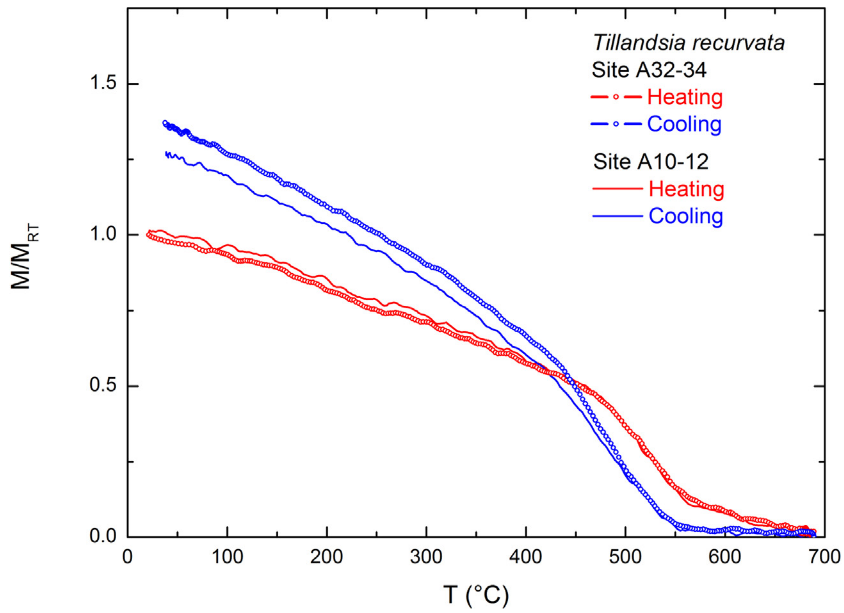

Fig. 3. Thermomagnetic curves for two selected samples from sites close to the industrial zone (A32-34) and the city center (A10-12) showing Curie temperatures close to that of magnetite. Units are arbitrary, M/M_{RT} indicate the relative magnetization compared to the initial one at room temperature.

Variations in magnetic grain sizes are also observed from the ratios κ_{ARM}/κ and ARM/SIRM, with coarser grains in polluted sites (see for example A1-3, A10-12, A19-21 and A32-34) compared to control sites (e.g., A22-24 and A41-43). This trend between magnetic concentration and grain size is also supported by significant correlation factors: $R = -0.556$, $p < 0.01$ for $\chi - \kappa_{ARM}/\kappa$; $R = -0.552$, $p < 0.01$ for χ-ARM/SIRM.

3.2. SEM observations and elemental content

Particles from *T. recurvata* differed in size, aspect and morphology depending on the degree of pollution, as shown by SEM and EDS analyses of 82 particles from six sites. Fig. 5a,b and d show Fe-rich irregularly spherical particles (ca. 2 μm) from sites A19-21 (high), A69-71 (moderate) and A22-24 (low pollution). Smaller spherules (about 1–2 μm and 1–3 μm) were found at the urban sites A19-21 and A47-49 (Fig. 5d and e, respectively) and industrial sites (A1-3, Fig. 5f). These latter sites had also irregular particles and wide size distribution (1–4 μm) and up to 20–40 μm for site A19-21.

Fe-rich particles are present in all sites, but its abundance increases in the following order: A19-21, A1-3, A38-40, A47-49, A69-71 and A22-24. The compositional analysis of EDS also revealed the presence of toxic elements: As (Fig. 5h), Sb (Fig. 5h), Cr, Mo (Fig. 5l), V, Zn (Fig. 5g), Ba (Fig. 5i), Hg (Fig. 5j), Pt (Fig. 5k), Cu (Fig. 5j), Au, Ce, Tb and Ta, which are product of urban/industrial contamination as reported in literature (Kukier et al., 2003; Thorpe and Harrison, 2008; Chaparro et al., 2010).

Most of these elements were found in site A19-21, close to an industrial area. Sites more affected by traffic pollution (A1-3, A47-49 and A69-71) show the presence of S, Mo, V, Zn, Ba, Hg, Cu (Fig. 5j) and Ce.

Elemental contents for all sites are detailed in a table as Supplementary data and the corresponding descriptive statistics is shown in Fig. 6. Most of the elements detected by EDS were confirmed and quantified by ICP-MS. Some elements of interest and

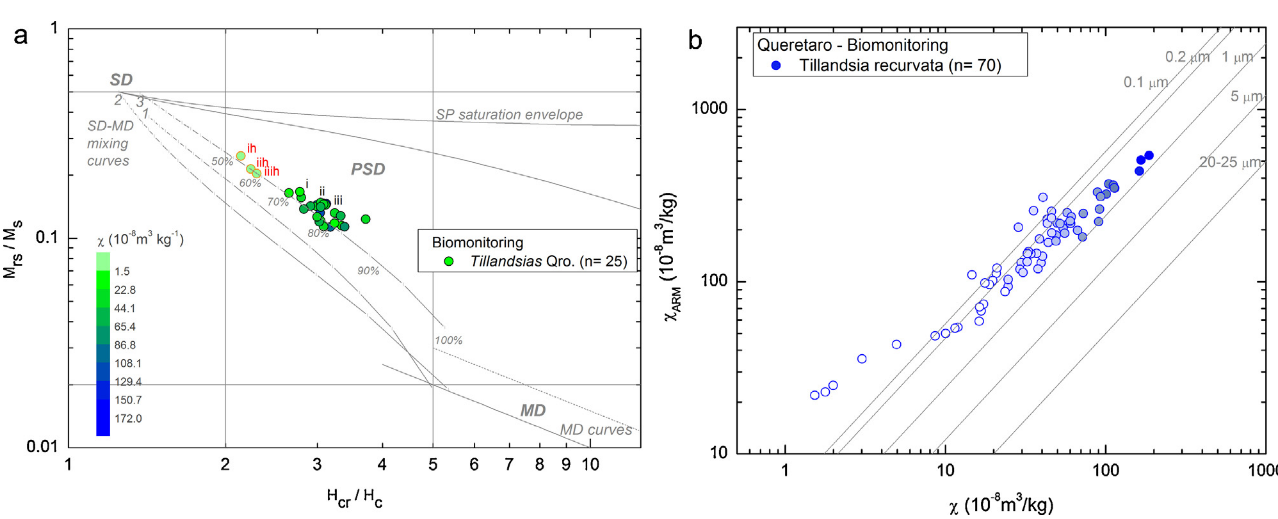

Fig. 4. (a) Day's plot (modified from Dunlop, 2002a,b), although all samples belong to the PSD region, if a mix between SD and MD grains are considered, MD(SD) concentrations are 70–85%; (b) King's Plot (χ_{ARM} versus χ) for all samples. Coarser magnetic grain sizes (about 1 μm) correspond to the most affected sited.

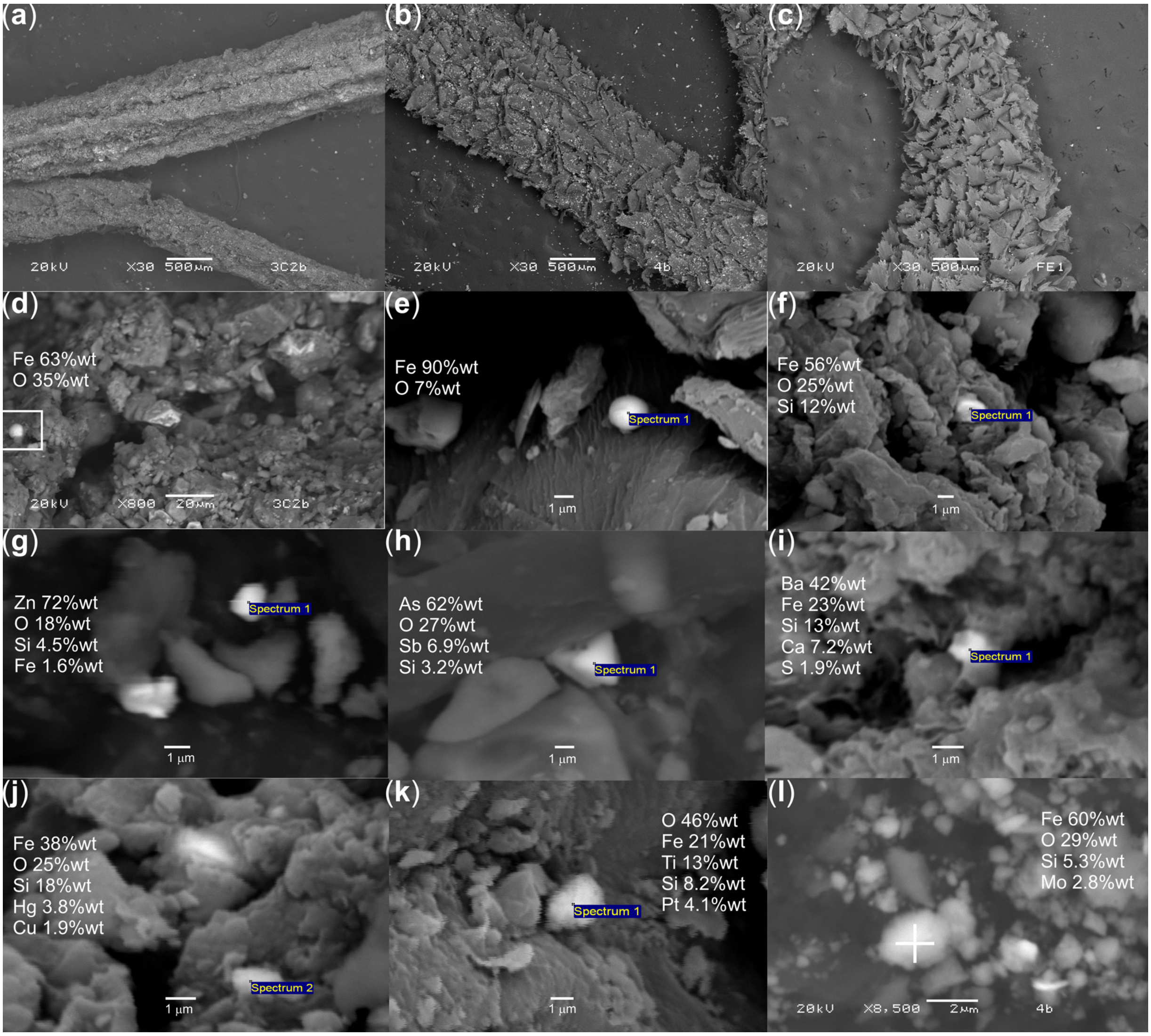

Fig. 5. SEM observations on *Tillandsias* samples with different pollution influence: (a) site A19-21 with dense population and high vehicular traffic, (b) site A69-71 with moderate vehicular traffic, (c) site A22-24 with low population and vehicular traffic. (d–e) Fe-rich spherules (about 2–3 μm) from sites A19-21 and A47-49 respectively. (f) Fe-rich irregular particle (∼2 μm) from site A1-3. Examples of: (g) Zn-rich irregular particle (∼1.5 μm) from site A19-21, (h) As-rich irregular particle (∼4 μm) with high Sb content from site A19-21, (i) Ba-rich irregular particle (∼1 μm) with high Fe and S contents from site A1-3, (j) Fe-rich irregular particle (∼2 μm) with high Hg and Cu contents from site A1-3, (k) Fe-rich irregular particle (∼2 μm) with high Ti and Pt content from site A38-40, (l) Fe-rich irregular particle (∼3 μm × 2 μm) with Mo content from site A69-71.

of adverse impact, e.g., Pb, Cr, V, Sn, Sb, Ba, Cu, Zn and Mo have been previously reported in studies using naturally grown specimens of *Tillandsia* spp. used for trace metal monitoring. Among them, Shacklette and Connor (1973) analyzed *Tillandsia usneoides* samples from southern USA including a wide variety habitats (roadsides, industrial and urban areas, forest locations, beaches and agricultural areas). They conclude that samples from industrial and highway locations are characterized by greater-than-average contents of As, Cd, Cr, Co, Cu, Pb, Ni and V. Most of the reported average element contents are lower than in our study, except for Pb.

Brighigna et al. (1997) studied *Tillandsia caput medusae* samples in San José (Costa Rica) where the main source of pollution is vehicular traffic, and they reported Pb (2–179 ppm) and Cu (2–69 ppm) values comparable to the present study. Schrimpff (1984) studied in situ *T. recurvata* samples in Cali and Medellín, the two largest cities (1.2 and 1.6 million inhabitants respectively, in 1981) in Colombia. He identified vehicular and industrial pollution sources; and the reported mean values for Zn (119 and 379 ppm), Pb (41 and 26 ppm), Cu (53 and 31 ppm), Ni (12 and 53 ppm) and Cr (26 and 124 ppm) are comparable to the Querétaro's values.

On the other hand, samples grown in situ in Querétaro show higher elemental contents compared to studies on transplanted *T. usneoides* (Pellegrini et al., 2014) and *Tillandsia capillaris* (Abril et al., 2014). Such differences may be explained by variations of the pollution loadings, as well as from different accumulation periods affecting the plants.

Average Cu values in rocks from our study area are 22 ppm (Mori et al., 2007). Sample A72-73 shows such a value, but most sites have higher values, ranging between 59 and 215 ppm, which are therefore associated to anthropogenic Cu-rich particles. The highest values correspond to A1-3, A32-34 and A64-66 (Supplementary data) and seem to be mainly produced by metallurgy industries (steel production). Among these particles, covellite (CuS), spherulites of Cu and Cu associated to Ni and Zn, are the most abundant ones.

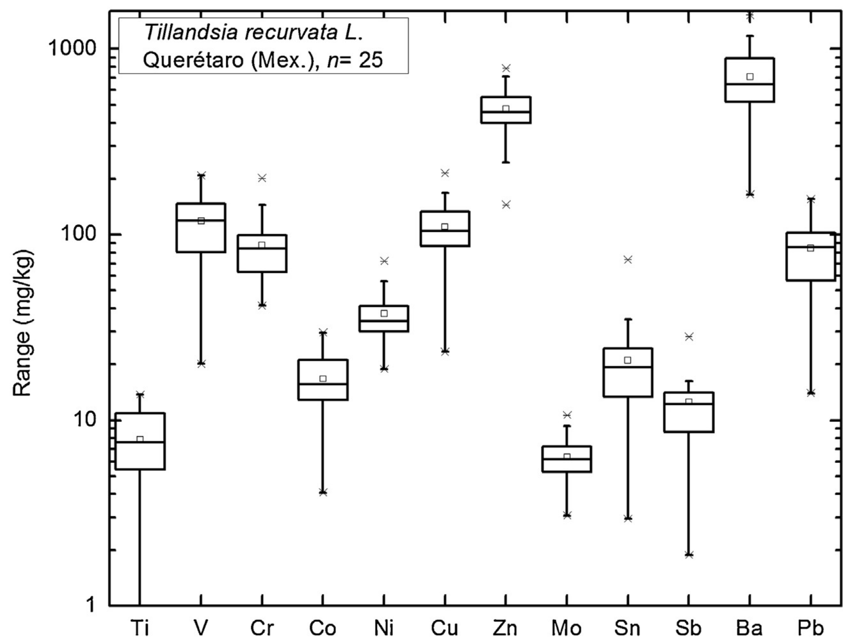

Fig. 6. Elemental composition of all sites ($n = 25$). Variability of some selected element contents (in mg/kg, except for Ti in g/kg). The box delineates interquartile range 25–75%, and the horizontal line in box indicates the median. Minimum and maximum values are shown using whiskers, as well as the mean value with an open square.

Antimony (Sb) is found in rocks from the study area with concentration of 0.03 ppm (Mori et al., 2007). Although similar or lower values were observed at some sites (e.g., A22-24 and A72-73), much higher concentrations of up to 29 ppm were observed in polluted sites, such as A1-3, A29-31, A32-34 and A64-66. The identified Sb particles were metallic antimony and antimony oxide (associated to Fe) which generally are not found in nature. Therefore, these particles also seem to be of anthropogenic origin, i.e., traffic-derived emissions (Weckwerth, 2001) and/or industrial activities (e.g., Arditsoglou and Samara, 2005). According to Pellegrini et al. (2014) several parts of vehicles contain Sb alloys and others Sb compounds.

Ba is found in rocks (in concentration between 270 and 800 ppm), but it has also been identified as an important tracer for vehicular activities (Monaci et al., 2000). Several Querétaro sites surpassed the natural concentration, with A1-3, A29-31, A32-34, A47-49 and A69-71 showing the highest concentrations (1003–1526 ppm). Both mineral ($BaSO_4$) and anthropic barium were observed from SEM–EDS. The latter is mainly generated by brake lining system wear (Chan and Stachowiak, 2004; Mosleh et al., 2004), as well as by industries related to the automobile sector and glass/pigment ($BaCO_3$) production.

Zn and Pb are present in rocks from the study area with concentrations of 88 ppm and 5 ppm, respectively (Mori et al., 2007). All sites show higher values of Zn and Pb than in nature, with A1-3, A32-34, A47-49, A50-52 and A64 -66 ranging between 628 and 787 ppm for Zn and between 109 and 155 ppm for Pb. Most of the identified Pb-rich particles have irregular form, which are metallic lead, lead oxide (most abundant), lead sulfide and some particles are associated to various elements: S, Sn, Sb, Cu and Fe. Zn and Pb particles can also come from multiples sources: vehicular traffic and industries.

Differences between sites are evident from detailed data (see the Supplementary data). Some of the elements of interest, such as Ba, Cu, Sb and Zn, have been reported as tracers of traffic-derived emissions (Amereih et al., 2005; Thorpe and Harrison, 2008) or industrial activities. According to Weckwerth (2001) and Arditsoglou and Samara (2005), the Cu/Sb concentration ratio is distinctive of vehicle-derived sources (Cu/Sb ∼ 5), metallurgical/cement industry activities (Cu/Sb > 10) or typical crustal rocks (Cu/Sb ∼ 125). Most of the polluted Querétaro sites have lower ratios of Cu/Sb about 6–11 than less affected sites.

3.3. Multivariate analysis

The samples were classified using FCC analysis but previously the bivariate statistical analysis (Pearson's correlation coefficients) was calculated. Significant correlations between magnetic and chemical variables are given in Table 1. Concentration-dependent magnetic parameters (χ, ARM, M_s and SIRM) are directly correlated with most of the elements (R between 0.400 and 0.653), being the most significant (at the 0.01 level) correlations with Sc, Ti, V, Cr, Co, Ni, Zn, Ga, Y, Zr, Mo, Sn, Sb, Ba and Pb. Direct significant correlations (R between 0.427 and 0.715) are also obtained between the parameters para/diamagnetic contribution and χ_{hf} with the elements: Be, Sc, Ti, V, Cr, Co, Ni, Cu, Zn, Ga, Sr, Y, Zr, Nb, Mo, Sn, Sb, Ba and Pb (Table 1). On the other hand, magnetic grain size-dependent parameters (κ_{ARM}/κ, ARM/SIRM and SIRM/χ) are inversely correlated (R between −0.398 and −0.676) with the elements. Among these parameters, ARM/SIRM has significant (at the 0.01 level) correlation with Sc, Ti, V, Co, Zn, Ga, Y, Zr, Mo, Sb and Pb.

It is interesting to note that significant correlations with trace elements such as V, Cr, Co, Zn, Sb, Mo and Pb have already been reported for vehicle-derived and industrial pollution studies. For vehicle-derived pollution studies, significant correlations between χ and Sb (Amereih et al., 2005), between SIRM and Pb (Maher et al., 2008) and between magnetic concentration parameters (χ and ARM) and elements Cr and Co (Marié et al., 2010) were reported. On the other hand, for industrial pollution, Zhang et al. (2011) found significant correlations between concentration-dependent magnetic parameters and V, Cr, Mo, Zn, Pb, Cd and Cu among other heavy metals.

Results corresponding to the fuzzy partition are detailed in Table 2 and represented in Fig. 7. Three clusters were determined by FCC and each sample was classified regarding its corresponding

Table 1
Bivariate statistical analysis for Tillandsias from Querétaro ($n = 25$).

	χ	ARM	SIRM	M_s	κ_{ARM}/κ	ARM/SIRM	SIRM/χ	Para/diamag. cont.	χ_{hf}
Li						−0.443*			
Be			0.420*	0.447*		−0.458*		0.469*	0.482*
Sc	0.516**	0.518**	0.575**	0.562**		−0.567**		0.522**	0.667**
Ti	0.565**	0.586**	0.630**	0.573**		−0.570**		0.553**	0.677**
V	0.490**	0.466*	0.541**	0.501*		−0.605**		0.438*	0.581**
Cr	0.604**	0.621**	0.617**	0.523**		−0.466*		0.549**	0.710**
Co	0.543**	0.543**	0.597**	0.542**		−0.585**		0.527**	0.674**
Ni	0.508**	0.510**	0.507**			−0.402*			0.478*
Cu						−0.437*		0.427*	0.505**
Zn	0.520**	0.416*	0.490*	0.439*	−0.485*	−0.621**		0.542**	0.603**
Ga	0.482*	0.512**	0.541**	0.557**		−0.512**		0.535**	0.616**
Sr						−0.482*			0.511**
Y	0.483*	0.505**	0.541**	0.603**		−0.533**		0.531**	0.630**
Zr	0.494*	0.522**	0.552**	0.565**		−0.520**		0.565**	0.622**
Nb	0.411*	0.456*	0.476*	0.549**		−0.483*		0.516**	0.574**
Mo	0.653**	0.519**	0.601**	0.489*	−0.610**	−0.676**	−0.447*	0.445*	0.577**
Sn	0.579**	0.569**	0.581**	0.530**	−0.398*	−0.501*		0.516**	0.715**
Sb	0.622**	0.505**	0.624**	0.452*	−0.499*	−0.670**		0.529**	0.670**
Ba	0.509**	0.458*	0.521**	0.430*		−0.486*		0.452*	0.639**
Tl		0.415*						0.456*	
Pb	0.540**	0.516**	0.570**	0.518**	−0.426*	−0.637**		0.480*	0.574**
U				0.400*				0.444*	

* Significant Pearson's coefficient at the 0.05 level is detailed.
** Significant Pearson's coefficients at the 0.01 level is detailed.

membership value (Fig. 7). In this graph, it is interesting to recognize the "transition" from F-cluster 1 characterized by higher magnetic and elemental concentrations to the F-cluster 3 with lower concentrations. Such discrimination can be noted in Table 2, where centroids for each F-cluster and for each variable accounted for it. The F-cluster 1 has the highest magnetic (i.e., χ, M_s, ARM and SIRM) and elemental concentrations opposed to F-cluster 3. In general, most of the sites show a clear difference in average concentration values, with samples from F-cluster 1 having centroid values about 2–3 times (for χ, ARM, SIRM, M_s, Pb, Cr, Co, Ni, Cu, Zn, V, Mo, Sn Sb and Ba) higher than the F-cluster 3 (sites with low pollution loading). These results show well-defined differences between groupings if concentration variables are taking into account.

Among magnetic mineral-dependent parameters, κ_{ARM}/κ ARM/SIRM and SIRM/χ show moderate differences indicating that coarser magnetic grains are associated to higher concentrations. However, the parameters para/diamagnetic contribution and χ_{hf} (calculated from hysteresis loops) also shows clear differences among F-clusters, being the paramagnetic contribution (to the ferromagnetic signal) dominant for high-concentration samples (F-cluster 1) and conversely, the diamagnetic contribution controls low-concentration samples (F-cluster 3).

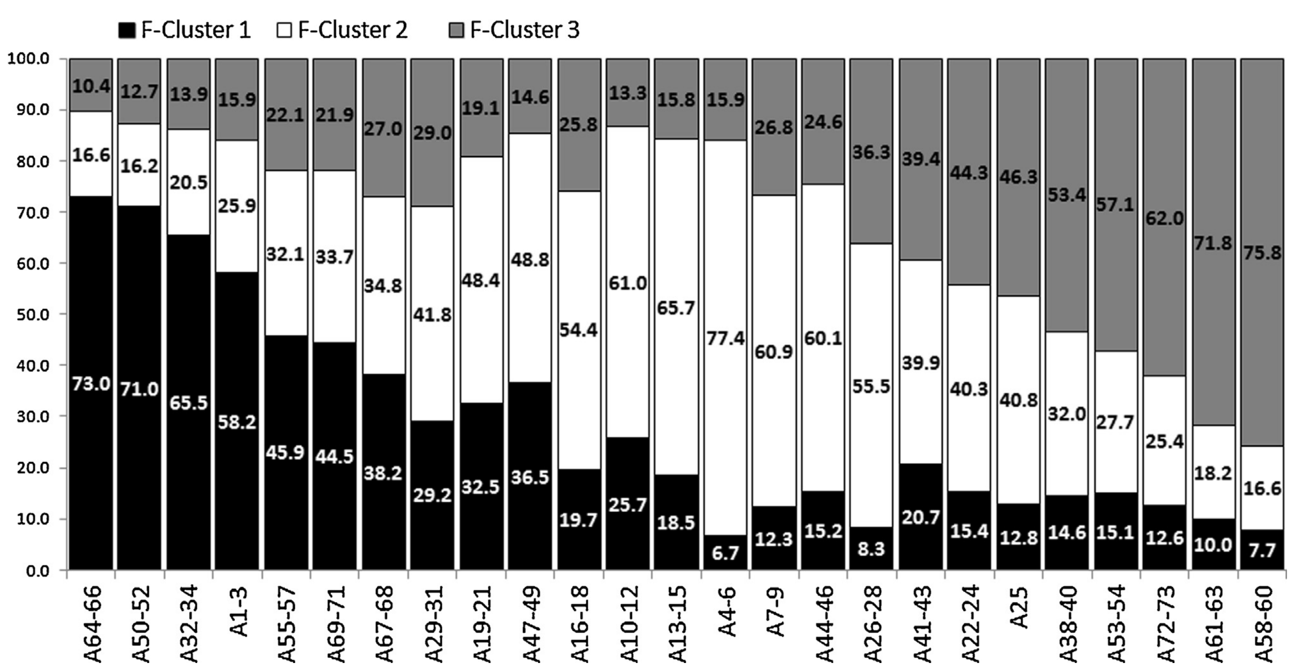

Fig. 7. Membership values for all samples from FCC analysis. Three F-clusters (using magnetic and chemical variables) are represented. The F-cluster 1 corresponds to the highest values of concentration-dependent magnetic and elemental variables.

Table 2
FCC analysis for 25 sites from Querétaro. Centroid values for each cluster are detailed.

Cluster	N	χ (10^{-8} m^3 kg^{-1})	ARM (10^{-6} A m^2 kg^{-1})	SIRM (10^{-3} A m^2 kg^{-1})	M_s (10^{-3} A m^2 kg^{-1})	κ_{ARM}/κ (dimensionless)	ARM/SIRM (dimensionless)	SIRM/χ (kA/m)	H_c (mT)	H_{cr} (mT)	H_{cr}/H_c (dimensionless)	M_r/M_s (dimensionless)	Para/diamag. cont. (%)
F-Cluster 1	7	83.2	198.9	13.8	433.7	3.58	0.0149	17.09	12.52	37.95	3.036	0.131	7.13
F-Cluster 2	11	36.1	100.0	6.3	109.9	4.90	0.0169	19.94	13.37	41.35	3.105	0.141	−1.75
F-Cluster 3	7	35.8	116.1	5.8	128.5	5.54	0.0211	18.67	12.26	37.76	3.094	0.131	−3.93

Cluster	N	χ_{hf} (10^{-8} m^3 kg^{-1})	Pb (mg/kg)	Cr (mg/kg)	Co (mg/kg)	Ni (mg/kg)	Cu (mg/kg)	Zn (mg/kg)	V (mg/kg)	Mo (mg/kg)	Sn (mg/kg)	Sb (mg/kg)	Ba (mg/kg)
F-Cluster 1	7	7.14	120.0	124.7	23.0	48.5	140.6	620.9	162.1	8.3	34.2	19.0	1015.1
F-Cluster 2	11	0.55	89.0	79.9	17.2	36.9	117.8	499.3	124.8	6.2	17.9	12.4	712.0
F-Cluster 3	7	0.59	42.0	63.4	9.7	27.3	67.8	290.4	63.6	4.6	12.6	6.2	390.7

3.4. Magnetic monitoring

Three parameters were selected from multivariate statistical studies and represented in Fig. 8 to investigate their spatial distribution: χ, κ_{ARM}/κ and χ_{hf}.

Magnetic susceptibility χ is one of the most used parameter in magnetic monitoring, as it is well-known, measurements are easy, prompt and cost-effective to carry out (Petrovský and Elwood, 1999). As proven by a great number of authors, it allows us to assess in a qualitative way the contamination of small scale areas (e.g., Kapicka et al., 1999; Chaparro et al., 2007; Zawadzki et al., 2012), as well as of large scale areas (e.g., Heller et al., 1998; Boyko et al., 2004; Blundell et al., 2009).

The distribution of mass specific susceptibility in Querétaro shows the highest values close to the industrial sites and principal traffic ways. These samples correspond to F-cluster 1 which is characterized by the highest magnetic and element concentrations. According to Fig. 8a, sites with high χ are closely grouped within a radius of about 1 km and most of the sites are associated to coarser magnetic grain sizes, i.e., lower κ_{ARM}/κ values (Fig. 8b).

Different to the low-field magnetic susceptibility, high-field magnetic susceptibility χ_{hf} is a parameter which is not commonly used in magnetic monitoring. Most of the magnetic monitoring studies have focused on χ because the ferrimagnetic contribution is mainly controlling the magnetic signal; however, additional or alternative magnetic parameters may have to be considered in different study cases (Chaparro et al., 2012). From statistical analyses, the χ_{hf} yields significant results with most elements; its distribution can be appreciated in Fig. 8c. As mentioned above, this parameter is associated with non-ferrimagnetic minerals, that is, mainly diamagnetic and paramagnetic minerals, but unsaturated antiferromagnetic minerals of high coercivity (e.g., hematite, goethite) may be also contributing. The χ_{hf} distribution reveals a clear difference between sites classified as F-cluster 1 with a paramagnetic contribution and F-cluster 3 sites (low pollution influence) with a predominant diamagnetic contribution.

Moreover, we observe a preferential distribution of high values of χ and χ_{hf} along the W–E/SW–NE direction; which agrees with the prevailing SW–NE wind direction for Querétaro during the winter season (in March, see Supplementary data). As mentioned, wind intensities and directions are also strongly seasonal, being from the E or NE about 37% of the year (INEGI, 2012).

In general, samples from F-cluster 2 (intermediate values of concentration and finer magnetic particle) are well distributed within the urban area, and most of the samples are in the city center and areas with high vehicular traffic, having moderate higher values of κ_{ARM}/κ (finer magnetic particles). Probably, these sites are affected by industrial and vehicle-derived pollutants with different magnetic grain size population. Although the discrimination between coarser/finer magnetic grains is of general interest, it is important to bear in mind that all estimated particle sizes <1 μm (Fig. 4b) are known to be harmful to the human health. According to samples A32-34, A50-52 and A19-21, a high concentration of coarser magnetic particles seems to come from the industrial area; however, these sites also have an important vehicular flux. The vehicular influence is clearly noted from some sites on (or close to) main streets and routes, such as, sites A1-3, A10-12, A16-18, A19-21 and A32-34.

Most of the sites (corresponding to F-clusters 1 and 2) show a clear difference in concentration values (Fig. 8a), where higher and relatively higher values are associated to areas with an important and continuous pollution loading (end-products emitted by industrial and traffic sources). While both pollution sources have to be considered, most of the highly polluted sites seem to be affected mainly by traffic-derived pollutants. This observation is supported

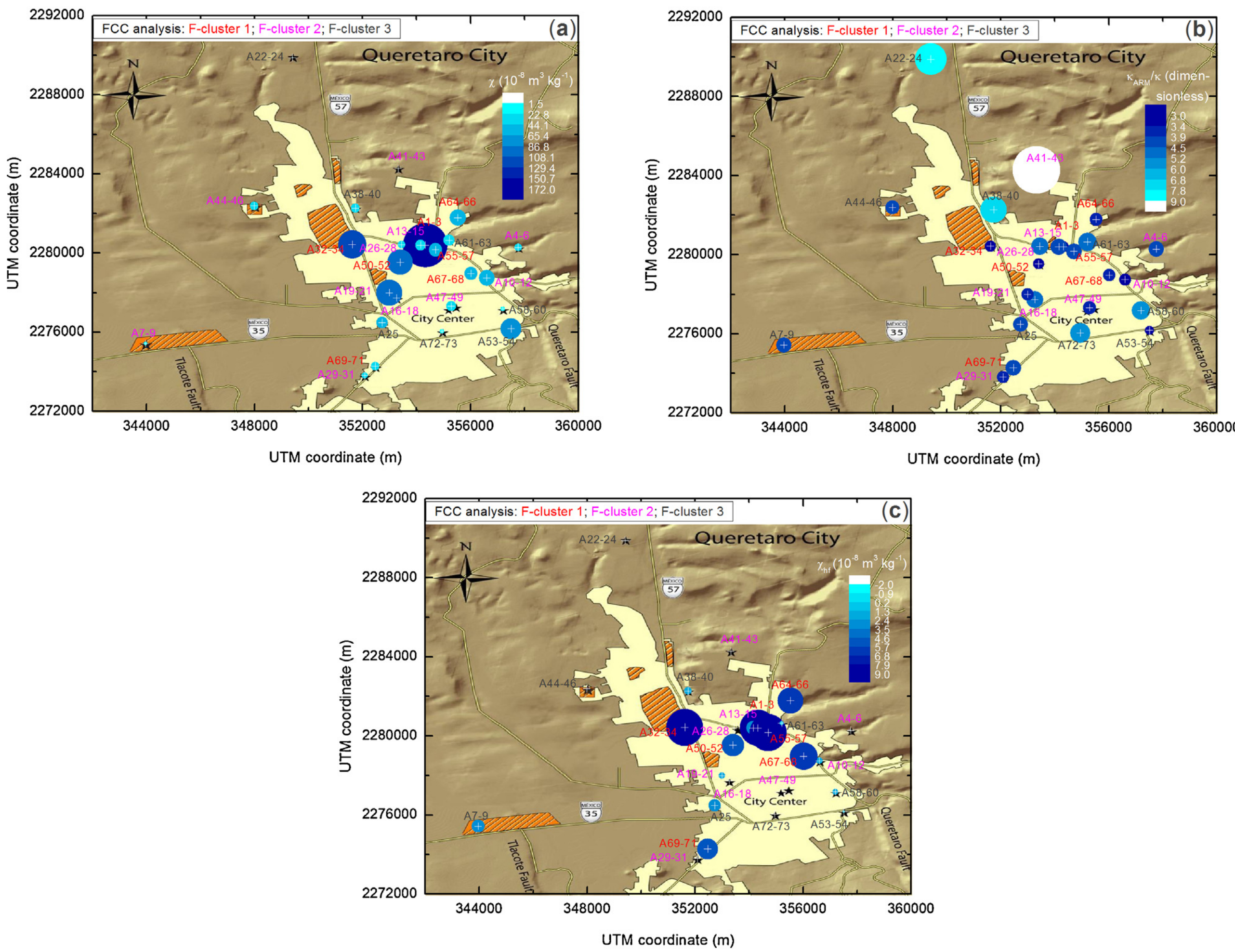

Fig. 8. Spatial distribution of (a) the concentration-dependent magnetic parameter: mass-specific susceptibility; and (b) the magnetic grain size-dependent parameter: κ_{ARM}/κ. (c) the high-field magnetic susceptibility parameter.

by data that highlight Cu and Sb as reliable tracers of non-exhaust particles from road traffic (Thorpe and Harrison, 2008).

4. Conclusion

The analysis of different magnetic parameters reveals the predominance of PSD magnetite or a corresponding mixture of SD and MD particles accumulated in *T. recurvata* L. Magnetic grains size estimations show the widespread presence of ultrafine and fine particles (<0.1–1 μm) which are breathable and harmful for health. The magnetic concentration dependent parameters show wide variations related to the influence of different pollution sources, i.e., industrial and urban activities, or their absence.

Multivariate analyses showed significant correlations between magnetic and trace elements of vehicle-derived and industrial particles that validate the use of magnetic parameters as proxies of pollution.

FCC analysis allowed classifying sites in three F-clusters with different pollution degree. It is observed that the paramagnetic contribution to the ferromagnetic signal is dominant for high-concentration samples (F-cluster 1) and the diamagnetic contribution controls low-concentration samples (F-cluster 3). Areas with important and continuous pollution loading (by industrial and/or traffic sources) show higher values of magnetic concentration and coarser magnetic grain sizes. Thus, it is important to not restrict the use of the magnetic susceptibility χ for monitoring just because its measurement is easy, prompt and cost-effective to carry out on *Tillandsias*, but also the complementary use of other magnetic parameters.

The magnetic and non-magnetic studies show that the *T. recurvata* is capable of intercept and collect atmospheric dusts in its diamagnetic matrix. Dusts collected by 7 high volume active air samplers with high instrument maintenance costs, with similar properties, were already reported by Castañeda-Miranda et al. (2014). This fact allows the inexpensive use of *Tillandsias* for future spatial and temporal biomonitoring in many places around the world where these species are present.

Acknowledgements

This research was partly supported by Posgrado en Ciencias de la Tierra (UNAM). The authors wish to thank the UNAM, UNCPBA and CONICET for their financial support. They also thank to the Lab Ultralimpio e ICP-MS (CGeo-UNAM), M.Sc. O. Pérez Arvizu for her technical support for ICP-MS studies, Marina Vega González for her help in the SEM studies and to Ing. J. Escalante for his help and support with the Curie balance. This manuscript was improved by useful suggestions of two anonymous reviewers.

Appendix A. Supplementary data

Supplementary data associated with this article can be found, in the online version, at http://dx.doi.org/10.1016/j.ecolind.2015.06.025

References

Abril, G.A., Wannaz, E.D., Mateos, A.C., Pignata, M.L., 2014. Biomonitoring of airborne particulate matter emitted from a cement plant and comparison with dispersion modelling results. Atmos. Environ. 82, 154–163.

Amereih, S., Meisel, T., Scholger, R., Wegscheider, W., 2005. Antimony speciation in soil samples along two Austrian motorways by HPLC-ID-ICP-MS. J. Environ. Monit. 7, 1200–1206.

Arditsoglou, A., Samara, C., 2005. Levels of total suspended particulate matter and major trace elements in Kosovo: a source identification and apportionment study. Chemosphere 59, 669–678.

Bermudez, G.M.A., Rodriguez, J.H., Pignata, M.L., 2009. Comparison of the air pollution biomonitoring ability of three *Tillandsia* species and the lichen *Ramalina celastri* in Argentina. Environ. Res. 109, 6–14.

Boyko, T., Scholger, R., Stanjek, H., MAGPROX TEAM, 2004. Topsoil magnetic susceptibility mapping as a tool for pollution monitoring: repeatability of in-situ measurements. J. Appl. Geophys. 55 (3–4), 249–259.

Böhm, P., Wolterbeek, H., Verburg, T., Mulisek, L., 1998. The use of tree bark for environmental pollution monitoring in the Czech Republic. Environ. Pollut. 102, 243–250.

Brighigna, L., Ravanelli, M., Minelli, A., Ercoli, L., 1997. The use of an epiphyte (*Tillandsia caput-medusae morren*) as bioindicator of air pollution in Costa Rica. Sci. Total Environ. 198, 175–180.

Blundell, A., Hannam, J.A., Dearing, J.A., Boyle, J.F., 2009. Detecting atmospheric pollution in surface soils using magnetic measurements: a reappraisal using an England and Wales database. Environ. Pollut. 157, 2878–2890.

Castañeda-Miranda, A.G., (Doctoral thesis) 2015. Caracterización y monitoreo magnético ambiental de partículas suspendidas en el aire urbano (Characterization and Magnetic Monitoring of Airborne Suspended Particles from an Urban Area). Universidad Nacional Autónoma de México.

Castañeda-Miranda, A.G., Böhnel, H., Molina-Garza, R., Chaparro, M.A.E., 2014. Magnetic evaluation of TSP-filters for air quality monitoring. Atmos. Environ. 96, 163–174.

Chan, D., Stachowiak, G.W., 2004. Review of automotive brake friction materials. Proc. Inst. Mech. Eng. 218 (D), 953–966.

Chaparro, M.A.E., Nuñez, H., Lirio, J.M., Gogorza, C.G.S., Sinito, A.M., 2007. Magnetic screening and heavy metal pollution studies in soils from Marambio station, Antarctica. Antarct. Sci. 19 (3), 379–393.

Chaparro, M.A.E., Marié, D.C., Gogorza, C.S.G., Navas, A., Sinito, A.M., 2010. Magnetic studies and scanning electron microscopy—X-ray energy dispersive spectroscopy analyses of road sediments, soils, and vehicle-derived emissions. Stud. Geophys. Geodaet. 54 (4), 633–650.

Chaparro, M.A.E., Chaparro, M.A.E., Sinito, A.M., 2012. An interval fuzzy model for magnetic monitoring: estimation of a pollution index. Environ. Earth Sci. 66 (5), 1477–1485.

Chaparro, M.A.E., Lavornia, J., Chaparro, M.A.E., Sinito, A.M., 2013. Biomonitors of urban air pollution: magnetic studies and SEM observations of corticolous foliose and microfoliose lichens and their suitability for magnetic monitoring. Environ. Pollut. 172, 61–69.

Correll, D.S., Johnston, M.C., 1970. Manual of the Vascular Plants of Texas. Texas Research Foundation, Renner.

Dunlop, D.J., 2002a. Theory and application of the Day plot (Mrs/Ms versus Hcr/Hc). 1. Theoretical curves and tests using titanomagnetite data. J. Geophys. Res. 107 (B3), 2056, http://dx.doi.org/10.1029/2001JB000486

Dunlop, D.J., 2002b. Theory and application of the Day plot (Mrs/Ms versus Hcr/Hc). 2. Application to data for rocks, sediments, and soils. J. Geophys. Res. 107 (B3), 2057, http://dx.doi.org/10.1029/2001JB000487

Fabian, K., Reimann, C., McEnroe, S.A., Willemoes-Wissing, B., 2011. Magnetic properties of terrestrial moss (*Hylocomium splendens*) along a north–south profile crossing the city of Oslo, Norway. Sci. Total Environ. 409, 2252–2260.

Fonseca, M.F., Bastos, W.R., Pinto, F.N., De, F., Rebelo, M., Torres, J.P.M., Guimaraes, J.R.D., Pfeifer, W.C., Marques, R.G., Malm, O., 2007. Can the biomonitor *Tillandsia usneoides* be used to estimate occupational and environmental mercury levels in the air? J. Braz. Soc. Ecotoxicol. 2 (2), 129–137.

Gasca, M., (Tesis) 2007. Caracterización por SEMEDS de aeropartículas antrópicas de la fracción respirable en la Ciudad de Querétaro y su relación con fuentes contaminantes. Universidad Autónoma de Qurératro.

Goix, S., Resongles, E., Point, D., Oliva, P., Duprey, J.L., de la Galvez, E., Ugarte, L., Huayta, C., Prunier, J., Zouiten, C., Gardon, J., 2013. Transplantation of epiphytic bioaccumulators (*Tillandsia capillaris*) for high spatial resolution biomonitoring of trace elements and point sources deconvolution in a complex mining/smelting urban context. Atmos. Environ. 80, 330–341.

Graciano, C., Fernández, L.V., Caldez, D.O., 2003. *Tillandsia recurvata* L. as a bioindicator of sulfur atmospheric pollution. Ecol. Austral 13, 3–14.

Heller, F., Strzyszcz, Z., Magiera, T., 1998. Magnetic record of industrial pollution in soils of Upper Silesia, Poland. J. Geophys. Res. 103 (B8), 17767–17774.

Instituto Nacional de Estadística Geográfica e informática 528 INEGI. 2006. Comunicado Núm. 108/06.

Instituto Nacional de Estadística Geográfica e informática INEGI. 2010. Censo Nacional de Población y Vivienda.

Instituto Nacional de Estadística Geográfica e informática INEGI. 2012. Perspectiva estadística Querétaro.

Jordanova, D., Petrov, P., Hoffmann, V., Gocht, T., Panaiotu, C., Tsacheva, T., Jordanova, N., 2010. Magnetic signature of different vegetation species in polluted environment. Stud. Geophys. Geod. 54, 417–442.

Kapicka, A., Petrovský, E., Ustjak, S., Machackova, K., 1999. Proxy mapping of fly-ash pollution of soils around a coal-burning power plant: a case study in Czech Republic. J. Geochem. Explor. 66, 291–297.

King, J., Banerjee, S.K., Marvin, J., Özdemir, Ö., 1982. A comparison of different magnetic methods for determining the relative grain size of magnetite in natural materials: some results from lake sediments. Earth Planet. Sci. Lett. 59, 404–419.

Kukier, U., Fauziah Ishak, C., Summer, M.E., Miller, W.P., 2003. Composition and element solubility of magnetic and non-magnetic fly ash fractions. Environ. Pollut. 123, 255–266.

Lehndorff, E., Urbat, M., Schwark, L., 2006. Accumulation histories of magnetic particles on pine needles as function of air quality. Atmos. Environ. 40, 7082–7096.

Madison, M., 1977. Vascular epiphytes: their systematic occurrence and salient features. Selbyana 2, 1–13.

Maher, B.A., Moore, C., Matzka, J., 2008. Spatial variation in vehicle-derived metal pollution identified by magnetic and elemental analysis of roadside tree leaves. Atmos. Environ. 42, 364–373.

Marié, D.C., Chaparro, M.A.E., Gogorza, C.S.G., Navas, A., Sinito, A.M., 2010. Vehicle-derived emissions and pollution on the road Autovia 2 investigated by rock-magnetic parameters: a case of study from Argentina. Stud. Geophys. Geod. 54, 135–152.

Monaci, F., Moni, F., Lanciotti, E., Grechi, D., Bargagli, R., 2000. Biomonitoring of airborne metals in urban environments: new tracers of vehicle emission, in place of lead. Environ. Pollut. 107, 321–327.

Moreno, E., Sagnotti, L., Dinares-Turell, J., Winkler, A., Cascella, A., 2003. Biomonitoring of traffic air pollution in Rome using magnetic properties of tree leaves. Atmos. Environ. 37, 2967–2977.

Mori, L., Gómez-Tuena, A., Cai, Y., Goldstein, S.L., 2007. Effects of prolonged flat subduction on the Miocene magmatic record of the central Trans-Mexican Volcanic Belt. Chem. Geol. 244, 452–473.

Mori, L., Gomez-Tuena, A., Schaaf, P., Goldstein, S.L., Perez-Arvizu, O., Solis-Pichardo, G., 2009. Lithospheric removal as a trigger for flood basalt magmatism in the Trans-Mexican volcanic belt. J. Petrol. 50 (11), 2157–2186.

Mosleh, M., Blau, P.J., Dumitrescu, D., 2004. Characteristics and morphology of wear particles from laboratory testing of disk brake materials. Wear 256, 1128–1134.

Muxworthy, A., Matzka, J., Petersen, N., 2001. Comparison of magnetic parameters of urban atmospheric particulate matter with pollution and meteorological data. Atmos. Environ. 35, 4379–4386.

Pellegrini, E., Lorenzini, G., Loppi, S., Nali, C., 2014. Evaluation of the suitability of *Tillandsia usneoides* L. as biomonitor of airborne elements in an urban area of Italy, Mediterranean basin. Atmos. Pollut. Res., http://dx.doi.org/10.5094/APR.2014.028

Petrovský, E., Elwood, B., 1999. Magnetic monitoring of air, land and water pollution. In: Maher, B.A., Thompson, R. (Eds.), Quaternary Climates, Environment and Magnetism. Cambridge University Press, pp. 279–322.

R version 2.15.0, 2012. The R Foundation for Statistical Computing. http://www.r-project.org/, ISBN 3-835900051-07-0.

Rzedowski, J., 1981. Vegetación de México (Vegetation in México). Editorial Limusa, México D.F., Mexico, 430 p.

Salo, H., Bucko, M.S., Vaahtovuo, E., Limo, J., Mäkinen, J., Pesonen, L.J., 2012. Biomonitoring of air pollution in SW Finland by magnetic and chemical measurements of moss bags and lichens. J. Geochem. Explor. 115, 69–81.

Sagnotti, L., Macri, P., Egli, R., Mondino, M., 2006. Magnetic properties of atmospheric particulate matter from automatic air sampler stations in Latinum (Italy): toward a definition of magnetic fingerprints for natural and anthropogenic PM10 sources. J. Geophys. Res. 111 (B12S22), http://dx.doi.org/10.1029/2006JB004508

Schrimpff, E., 1984. A pollution patterns in two cities of Colombia, South America, according to trace substances content of an epiphyte (*Tillandsia recurvata* L.). Water Air Soil Pollut. 21, 279–315.

Shacklette, H.T., Connor, J.J., 1973. Airborne Chemical Elements in Spanish Moss, Geol. Survey Profess. Papers 574-E. U.S. Government Printing Office, Washington, pp. 46.

Secretaria de Desarrollo Sustentable, SEDESU, 2006. Anuario Económico de Querétaro, Available at: http://www.queretaro.gob.mx/sedesu/deseco/esteco/perfeco/anuario/2006/index.htm

Secretaria de Desarrollo Sustentable, SEDESU, 2011. Anuario Económico del estado de Querétaro.

Shu, J., Dearing, J.A., Morse, A.P., Yu, L., Yuan, N., 2001. Determining the sources of atmospheric particles in Shanghai, China, from magnetic and geochemical properties. Atmos. Environ. 35, 2615–2625.

Thorpe, A., Harrison, R.M., 2008. Sources and properties of non-exhaust particulate matter from road traffic: a review. Sci. Total Environ. 400, 270–282.

Weakley, A., 2010. Flora of the Southern and Mid-Atlantic States. University of North Carolina Herbarium, pp. 161.

Weckwerth, G., 2001. Verification of traffic emitted aerosol components in the ambient air of Cologne (Germany). Atmos. Environ. 35 (32), 5525–5536.

Xie, S., Dearing, J.A., Boyle, J.F., Bloemendal, J., Morse, A.P., 2001. Association between magnetic properties and element concentrations of Liverpool street dust and its implications. J. Appl. Geophys. 48, 83–92.

Zawadzki, J., Magiera, T., Fabijanczyk, P., Kusza, G., 2012. Geostatistical 3-dimensional integration of measurements of soil magnetic susceptibility. Environ. Monit. Assess. 184, 3267–3278.

Zhang, C.X., Huang, B.C., Piper, J.D.A., Luo, R.S., 2008. Biomonitoring of atmospheric particulate matter using magnetic properties of *Salix matsudana* tree ring cores. Sci. Total Environ. 393, 177–190.

Zhang, C., Qiaoa, Q., Piper, J.D.A., Huang, B., 2011. Assessment of heavy metal pollution from a Fe-smelting plant in urban river sediments using environmental magnetic and geochemical methods. Environ. Pollut. 159, 3057–3070.